sciendo DOI: 10.2478/ace-2018-0043 ARCHIVES OF CIVIL ENGINEERING
Vol. LXIV ISSUE 4 2018

THEORETICAL ANALYTICAL SOLUTION OF DEFORMATION AND STRESS DISTRIBUTION OF UNDERGROUND GAS STORAGE CAVERN IN BEDDED SALT ROCK

P. XIE[1], H. J. WEN[2], G. J. WANG[3], J. Hu[4]

Abstract: The main purpose of the study is to investigate the mechanical properties around an underground gas storage cavern in bedded salt rock. Firstly, considering the characteristics of the salt rock formation in China, the mechanical model was simplified into a hollow cylinder, which containing non-salt interlayer. In terms of elastic theory, Love displacement function was developed, and the elastic general solution of stress and deformation components were obtained after determining the undetermined coefficients. Under the same condition, numerical simulation was carried out. The validity of the elastic general solution is verified by comparing to numerical simulation results. Furthermore, Based on the feasible general elastic solution, viscoelastic solution was obtained through Laplace transformation and inverse Laplace transform, which could provide reference for the study on the stability and tightness of underground gas storage carven during operation to some extent.

Keywords: Bedded salt rock, Theoretical analysis, Love displacement function, Elastic-viscoelastic correspondence principle, Three-dimensional explicit finite-difference

[1] PhD., Eng., Chongqing University, Faculty of Civil Engineering, ChongQing 400045, China, e-mail: 526458865@qq.com
[2] Prof., DSc., PhD., Eng., Chongqing University, Faculty of Civil Engineering, ChongQing 400045, China, e-mail: 32943982@qq.com
[3] Prof., DSc., PhD., Eng., Hebei University of Technology, Faculty of Civil Engineering, Tianjian 300401, China, e-mail: dongshanxiaopeng@163.com
[4] PhD., Eng., Chongqing University, Faculty of Civil Engineering, ChongQing 400045, China, e-mail: 347902268@qq.com

1. INTRODUCTION

Energy reserve is the important guarantee for rapid economy development. Underground storage is safe and economic, so 60% of the storage facilities are located in subsurface in the world. Salt rock has certain distinctive properties, including very low permeability, wide distribution and so on [1-4], which is regarded as the ideal medium for gas storage, and salt rock caverns are widely used in many countries. According to statistics, about 554 underground salt rock gas storage caverns were in operation around the world by the end of 2012 [5]. Generally speaking, ideally underground gas storages are constructed in salt domes or diapirs [6-8]. Moreover, salt rock formations in China are usually layered structure with many alternating layers (rock salt, anhydrite or mudstone), and the geometric extent of the salt beds is large in the horizontal direction but small in the vertical direction [9]. In recent years, the related construction of deep salt rock storage cavern is developing vigorously in China. Although salt rock cavern is relatively safer than other storages, a series of catastrophic accidents (leakage of oil/gas, ground surface subsidence and salt rock cavern failure) frequently happen since 1950s, which led to fatal losses in human life and properties. Scholars' extensive attentions were paid to the properties of different types of salt caverns.

In the past few years, the related researches on the mechanical properties and stability of salt rock cavern have been conducted. For the properties of salt rock, elastic modulus, shear modulus and so on were seen as the important parameters of salt rock [10]. The physical and mechanical properties of heated salt rock were investigated [11-12]. The deformation behavior, strength and damage of salt rock subjected to cyclic loading were presented under confining pressure condition, using TAW–2000 computer-servo rock triaxial testing machine [13]. In order to study the stability of gas storage cavern， M-D model was proposed to describe creep of salt rock affected by rheology [14]. Expanded boundary and expanded damage criterion was presented through experimental study respectively [15-16]. The effect of stress and temperature on creep of salt rock was affected [17-18]. On the basis of laboratory creep test result of salt rock, a nonlinear constitutive model and damage evolution equation was suggested [19]. In China, the salt rock formation is characterized by containing non-salt interlayer. Due to the differences in tectonic structure and actual geological conditions, non-salt interlayer affected the deformation and failure characteristics of storage cavern. An analysis of the influence of interlayer was made based on Cosserate medium expending theory [20]. For 3 typical kind of interlayer in china, the deformation and failure characteristics of salt rock with tilted unsalted interlayer were revealed [21-22]. With the development of technology, FEM, artificial intelligence methods and reliability were introduced in the study of the stability of gas storage cavern [23-26].

In summary, the study on salt rock gas storage cavern was carried out in many aspects, and a large number of achievements were obtained. However, as for three-dimensional theoretical analytical solution is relatively bare. In this paper, considering the characteristics of the salt rock formation in China, mechanical model was simplified into a hollow cylinder with interlayer, which containing non-salt interlayer. In terms of elastic theory, the elastic general solution was solved. Under the same condition, numerical simulation was carried out. The validity of the elastic general solution is verified by comparing to numerical simulation results, which shows the elastic general solution could describe the mechanical characteristics of gas storage cavern in bedded salt rock in elasticity stage well. Furthermore, based on the feasible general elastic solution, viscoelastic solution was obtained through Laplace transformation and inverse Laplace transform, which could provide reference for the study on the stability and tightness of underground energy storage carven during operation to some extent.

2. MECHANICAL MOSEL OF STORAGE CAVERN IN BEDDED SALT ROCK

Due to salt rock can be easily dissolved in water, the gas storage caverns are mainly formed through aqueous fusion method [27]. The process is as follows (Fig. 1): Firstly, a pilot is drilled from surface to the predetermined posit in the bedded salt rock (Ⅰ). Secondly, Fresh water or unsaturated brine is injected into the cavity through the inner leaching tube (or through the annulus between the inner and outer leaching tubes) (Ⅱ). Finally, high concentration brine is ejected to the surface through the annulus between the inner and outer leaching tubes (or through the inner leaching tube) (Ⅲ). The ratio of radius and height is relatively small for gas storage cavern formed through aqueous fusion method [27]. In addition, considering the characteristics of the salt rock formation in China, the mechanical model was simplified into a hollow cylinder, which containing non-salt interlayer (Fig. 2).

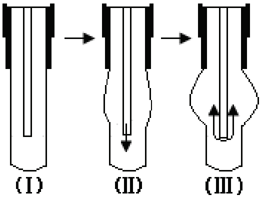

Fig. 1. The process of aqueous fusion method.

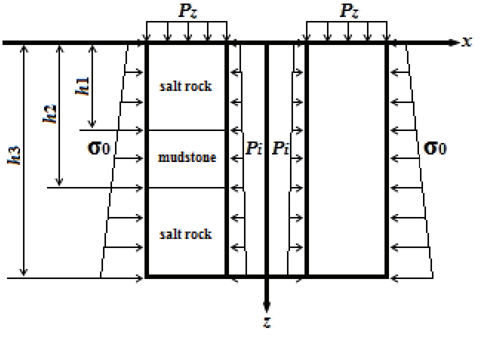

Fig. 2. The mechanical model for theoretical analysis.

The parameters in Fig. (2) are

p_z——the overburden load;

p_i ——the internal pressure of the cavern;

σ_0 ——initial horizontal stress

γ_0——the weighted mean specific weight of the overburden of the considered point;

γ_g——the specific weight of the stored medium in the cavern;

a ——radius of the storage cavern;

h_1, h_2, h_3 ——the depth of the strata.

According to the relevant literature and actual condition, the boundary conditions for this problem are [22] [29][31]:

(1) $z=0$, $\sigma_z = p_z$;

(2) $z = h_3$, $w = 0$, that means that there is no vertical displacement at the reference bottom plane of the model;

(3) $r = a$, $\sigma_r = p_i = p_0 + \gamma_g z$, internal pressure considering the gravity of the stored medium of the cavern;

(4) $r \to \infty$, $\sigma_r = \sigma_0 = \frac{\mu}{1-\mu}(\gamma_0 z + p_z)$;

(5) $r \to \infty$, $u = 0$;

The continuity conditions for this problem are [28]:

(1) $z = h_i$, $u_i = u_{i+1}$, that means the continuity of the radial displacement at the interface between salt rock and mudstone;

(2) $z = h_i$, $w_i = w_{i+1}$, that means the continuity of the vertical displacement at the interface between salt rock and mudstone;

(3) $z = h_i$, $\sigma_{zi} = \sigma_{zi+1}$, that means the continuity of the vertical stress at the interface between salt rock and mudstone;

where p_0——the internal pressure at the upper surface of the model;

i ——serial number of the strata, $i = 1, 2, 3$ in the model.

3. ELASTIC ANALYSIS

3.1 THE BASIC THEORY

In order to carry out systematic theoretical studies, the major assumptions for the established model are [29]:

(1) The matter of an elastic body is homogeneous

(2) The matter of an elastic body is continuously distributed over its volume so that the smallest element cut from the body possesses the same specific physical properties as the body

(3) The body is isotropic, that the elastic properties are the same in all directions

Considering the gravity, the equilibrium differential equations for the spatial axisymmetric problem are [29]

$$\left.\begin{aligned}\frac{\partial\sigma_r}{\partial r}+\frac{\partial\tau_{zr}}{\partial z}+\frac{\sigma_r-\sigma_\theta}{r}=0\\ \frac{\partial\sigma_z}{\partial z}+\frac{\partial\tau_{zr}}{\partial r}+\frac{\tau_{zr}}{r}-\gamma_0=0\end{aligned}\right\} \tag{1}$$

For the spatial axisymmetric problem, the displacement and stress components are shown [29]

$$\left.\begin{aligned}u&=-\frac{1}{2G}\frac{\partial^2}{\partial r\partial z}\varphi(r,z)\\ w&=\frac{1}{2G}\left[2(1-\mu)\nabla^2-\frac{\partial^2}{\partial z^2}\right]\varphi(r,z)\\ \sigma_r&=\frac{\partial}{\partial z}(\mu\nabla^2-\frac{\partial^2}{\partial r^2})\varphi(r,z)\\ \sigma_\theta&=\frac{\partial}{\partial z}(\mu\nabla^2-\frac{1}{r}\frac{\partial}{\partial r})\varphi(r,z)\\ \sigma_z&=\frac{\partial}{\partial z}[(2-\mu)\nabla^2-\frac{\partial^2}{\partial z^2}]\varphi(r,z)\\ \tau_{zr}&=\frac{\partial}{\partial r}[(1-\mu)\nabla^2-\frac{\partial^2}{\partial z^2}]\varphi(r,z)\end{aligned}\right\} \tag{2}$$

where ∇^2 is Laplace operator,

$$\nabla^2=\frac{\partial^2}{\partial r^2}+\frac{1}{r}\frac{\partial}{\partial r}+\frac{\partial^2}{\partial z^2}$$

3.2 The elastic general solution

According to basic elastic theory, the Love displacement function was established, which consists of polynomial and logarithmic functions [29]:

$$\varphi=(B_iz^2+C_ir^2+D_iz)\cdot\ln r+A_iz^3+F_iz^4+Mr^2+Nz^2$$

(3)

where A_i, B_i, C_i, D_i, F_i, M, N are the undetermined coefficients

Substituting Eq. (3) into Eq. (2) leads to

$$u = -\frac{1}{2G_i}\frac{2 \cdot B_i z + D_i}{r} \tag{4}$$

$$w = \frac{1}{G_i}\{[(1-2\mu_i)B_i + 4C_i(1-\mu_i)]\cdot \ln r + 4(C_i + M)(1-\mu_i) + (3A_i z + 6F_i z^2 + N)(1-2\mu_i)\} \tag{5}$$

$$\sigma_r = 6A_i\mu_i + 24F_i\mu_i z + \frac{2B_i z + D_i}{r^2} \tag{6}$$

$$\sigma_\theta = 6A_i\mu_i + 24F_i\mu_i z - \frac{2B_i z + D_i}{r^2} \tag{7}$$

$$\sigma_z = (6A_i + 24F_i z)(1-\mu_i) \tag{8}$$

$$\tau_{rz} = \frac{4C_i(1-\mu_i) - 2B_i\mu_i}{r} \tag{9}$$

where μ_i, G_i are the elastic parameters of the material.

The stress components in Eqns. (6)-(9) are proved to satisfy the equilibrium differential equations (1).

Considering the boundary conditions (3) and (4), the radial stress can be expressed by

$$\sigma_{r|r=a} = 6\mu_i A_i + 24\mu_i F_i z + \frac{2B_i z + D_i}{a^2} = p_0 + \gamma_g z \tag{10}$$

$$\sigma_{r|r\to\infty} = 6\mu_i A_i + 24\mu_i F_i z = \frac{\mu_i}{1-\mu_i}(\gamma_0 z + p_z) \tag{11}$$

Comparing the both sides of the above equations leads to

$$\left.\begin{aligned} A_i &= \frac{p_z}{6(1-\mu_i)} \\ F_i &= \frac{\gamma_0}{24(1-\mu_i)} \end{aligned}\right\} \tag{12}$$

$$\left.\begin{aligned} B_i &= \frac{a^2}{2}\left(\gamma_g - \gamma_0\frac{\mu_i}{1-\mu_i}\right) \\ D_i &= a^2\left(p_0 - p_z\frac{\mu_i}{1-\mu_i}\right) \end{aligned}\right\} \tag{13}$$

To ensure the condition of limited value, the term lnr in Eq. (5) should not exist, the coefficients B_i and C_i should therefore meet the relationship as follows

$$C_i = -\frac{1-2\mu_i}{4(1-\mu_i)}B_i \tag{14}$$

that is

$$C_i = \frac{1-2\mu_i}{4(1-\mu_i)}\frac{a^2}{2}\left(\frac{\mu_i}{1-\mu_i}\gamma_0 - \gamma_g\right) \tag{15}$$

Eq. (5) and Eq. (9) can be rewritten as

$$w = \frac{1}{G_i}[(1-2\mu_i)(3A_i z + 6F_i z^2 + N) + 4(1-\mu_i)(C_i + M)] \tag{16}$$

$$\tau_{rz} = -B_i / r \tag{17}$$

Substituting continuity conditions (2) into Eq. (16)

$$\left.\begin{array}{l} [(1-2\mu_1)(3A_1h_1 + 6F_1h_1^2 + N) + 4(1-\mu_1)(C_1 + M)]/G_1 = \\ [(1-2\mu_2)(3A_2h_1 + 6F_2h_1^2 + N) + 4(1-\mu_2)(C_2 + M)]/G_2 \\ [(1-2\mu_2)(3A_2h_2 + 6F_2h_2^2 + N) + 4(1-\mu_2)(C_2 + M)]/G_2 = \\ [(1-2\mu_3)(3A_3h_2 + 6F_3h_2^2 + N) + 4(1-\mu_3)(C_3 + M)]/G_3 \end{array}\right\} \tag{18}$$

Based on the solved coefficients in Eq. (12), Eq. (13) and Eq. (15), the undetermined coefficients M, N are given

$$\left.\begin{array}{l} M = \dfrac{T_2(3V_1h_1 + 6X_1h_1^2 + 4Y_1)}{4(T_2S_1 - T_1S_2)} - \dfrac{T_2(3V_2h_2 + 6X_2h_2^2 + 4Y_2)}{4(T_2S_1 - T_1S_2)} \\ N = \dfrac{T_2(3V_1h_1 + 6X_1h_1^2 + 4Y_1)}{T_2S_1 - T_1S_2} - \dfrac{S_2T_1(3V_2h_2 + 6X_2h_2^2 + 4Y_2)}{T_2(T_2S_1 - T_1S_2)} \\ \qquad - \dfrac{3V_2h_2 + 6X_2h_2^2 + 4Y_2}{T_2} \end{array}\right\} \tag{19}$$

where

$$\left.\begin{array}{l} S_n = O_n - K_nR_{n+1} \\ T_n = L_n - K_nL_{n+1} \\ V_n = K_nQ_{n+1} - Q_n \\ X_n = K_nR_{n+1} - R_n \\ Y_n = K_nP_{n+1} - P_n \\ K_n = G_n / G_{n+1} \\ O_n = 1 - \mu_n \\ L_n = 1 - 2\mu_n \\ P_n = O_nC_n \\ Q_n = L_nA_n \\ R_n = L_nF_n \\ n = 1, 2 \end{array}\right\}$$

Then, the elastic general solution was obtained:

When serial number of the strata is 1: i=1.

When serial number of the strata is 2: i=2.

When serial number of the strata is 3: i=3.

3.3 Comparison of elastic solution and numerical simulation

Fig. 3 is the calculation model for numerical simulation, the radius of the cavern is 20m. The lateral boundaries are placed 120m away from the carven center, and the depth ranges from 0m to 230m. There is 5m thickness interlayer in the depth of 120m. Table 1 lists the parameters of calculation model.

Table 1. The parameters of calculation model

Parameter / Serial number	γ_1(kN/m^3)	γ_{01}(kN/m^3)	γ_q(kN/m^3)	P_i(MPa)	p_z(MPa)	μ_1	E_1(GPa)
1	23	23	7.026	6	30	0.3	18
2	26.5	23.14	7.026	6	30	0.25	20.4
3	23	23.08	7.026	6	30	0.3	17.6

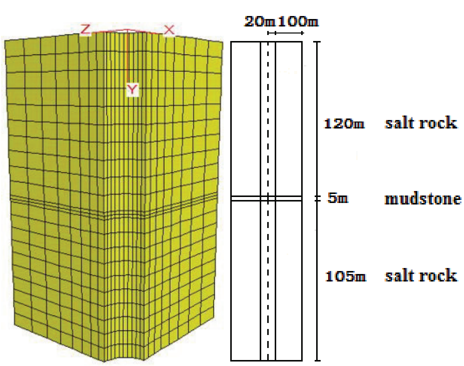

Fig. 3. Calculation model for numerical simulation

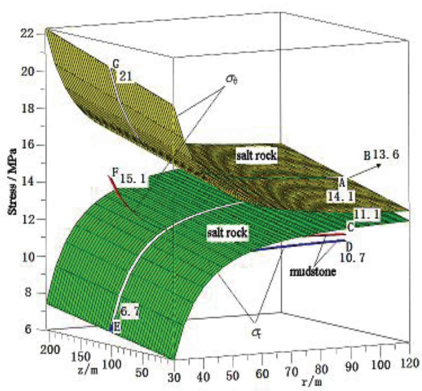

Fig. 4. Stress distribution (internal pressure p_i = 6MPa)

The radius stress and circumferential stress were derived from Eq. (6) and Eq. (7). The 3D diagram of radius stress and circumferential stress were plotted using Maple 14 software (Fig. 4), which represent the trend of radius stress and circumferential stress change. The distribution of radius stress and circumferential stress are all similar to paraboloid, and the value tends to content finally. However, the trend of value change for radius stress and circumferential stress are opposite with the change of radius and depth. Taking the depth is 100 m as an example, the value of radius increases from 6.7MPa to 13.6MPa, and the value of circumferential stress decreases from 21MPa to 11.1Mpa (point A). The rate of value change is consistent

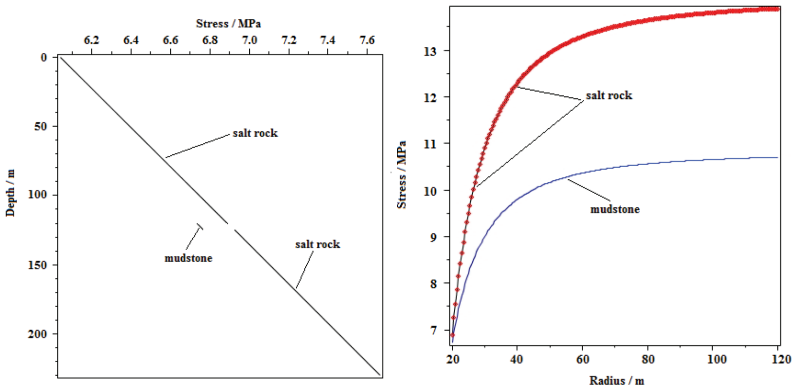

(a) (b)

Fig. 5. The planar diagram of radial stress

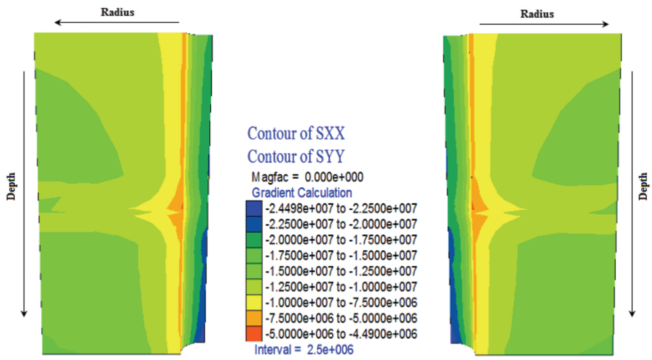

Fig. 6. The counter of radial stress

Taking radius stress as an example to evaluate the calculation results in qualitative. When the value of radius and depth are constants respectively(r=20, z=120), the planar diagrams of radius stress were presented in Fig. 5((a) and (b)). It is found that the relationship between radius stress and depth is linear (Fig. 5(a)), and the continuity is lost in the interlayer. The values of change are 0.1563MPa and 0.1564MPa at the upper and lower of the non-salt interlayer surface, accordingly the rate of change are 2.23% and 2.2%. Fig.5 (b) shows the trend of radius stress change is in the same for salt rock and non-salt rock interlayer, and there is some difference in value because of different properties of materials. Under the same condition, numerical simulation was finished, and the counter of radial stress is presented in Fig. 6. When the radius is 20m, the value of radial stress ranges from 5MPa to 10MPa. When the depth is 120m, the value of radial stress varies from 5MPa to 15MPa. The theoretical calculation results are consistent with the numerical simulation results.

Fig. 7 is the planar diagram of vertical stress. The value of vertical stress increase with the increase of the depth, and the distribution of vertical is continuous. Fig. 8 is the counter of vertical stress, obtained through numerical simulation, and the value change is consistent with the gravity effect. The theoretical calculation results matches well with the numerical simulation results.

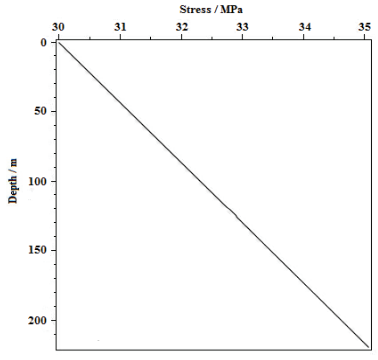

Fig. 7. The planar diagram of vertical stress

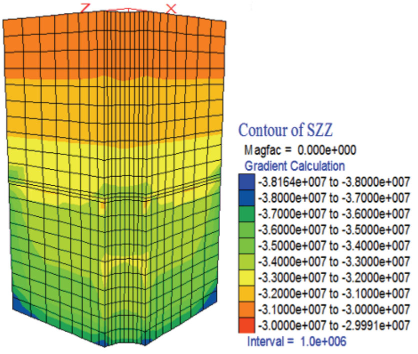

Fig. 8. The counter of vertical stress

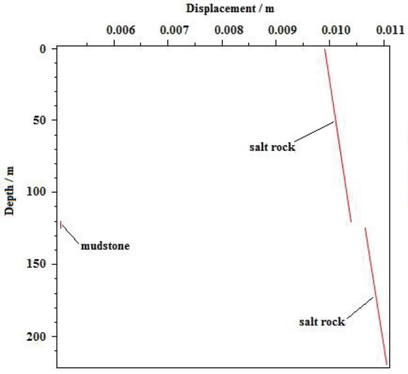

(a)

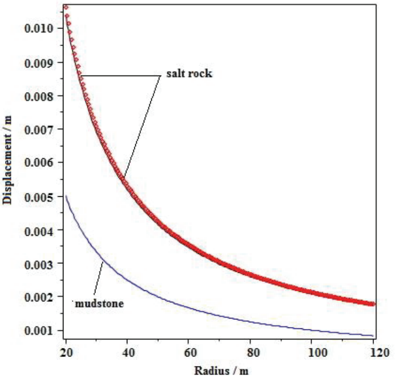

(b)

Fig. 9. The planar diagram of radial displacement

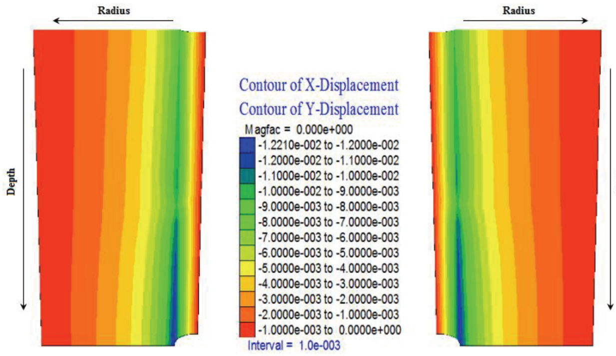

Fig. 10. The counter of radial displacement

The radial displacement was computed by Eq. (4), radius and depth are the two influencing factors of its value. When the value of radius and depth are constants respectively(r=20, z=120), the planar diagrams of radial displacement are presented in Fig. 9(a) and Fig. 9(b). The diagrams indicate the radial displacement lost continuity condition at the non-salt layer, which matches well with the numerical simulation results (Fig.10). Beside, the maximum value of change is only 3.9643mm, which meet the requirement of storage cavern design analysis.

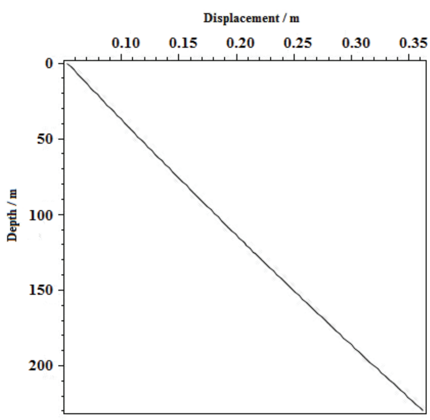

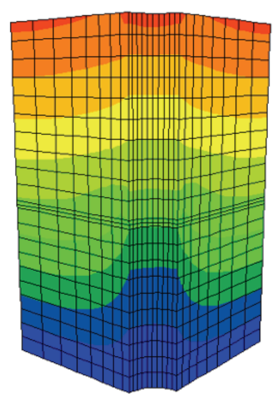

Fig. 11.The planar diagram of vertical displacement

Fig. 12. The diagram of vertical displacement

The curve of vertical displacement is a straight line in Fig. 11, the continuity condition was met. Fig. 12 was obtained through numerical simulation, which presents the vertical displacement is continuous.

The comparison of elastic solution and numerical simulation shows a good agreement, which indicates the elastic solution can describe the mechanical characteristics of this kind of gas storage cavern in bedded salt rock in elasticity stage well.

4. VISCOELASTIC ANALYSIS

In order to study the mechanical properties of rock, the stress-strain curves were drawn by Miller after uniaxial tests of 28 kinds of rock [31].The characteristics of the stress-strain curves, indicates salt rock is viscoelastic material. Based on elastic-viscoelastic correspondence principle, viscoelastic solution can be achieved by Laplace and inverse Laplace transform [30]. Modified Kelvin model was chosen as the viscoelastic model (Fig. 13).

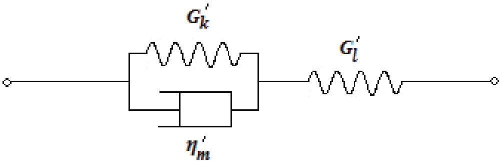

Fig. 13. Modified Kelvin model

Where G_l' — shear modulous

G_k' — Kelvin shear modulous

η_m' — kelvin viscosity

The constructive equation of Modified Kelvin model is [21]

$$S_{ij} + p_1' Si_j = q_0' e_{ij} + q_1' e_{ij} (q_1' > p_1' q_0') \tag{20}$$

Where $p_1' = \frac{\eta_m'}{G_l' + G_k'}$、$q_0' = \frac{2G_l' G_k'}{G_l' + G_k'}$、$q_1' = \frac{2G_k' \eta_m'}{G_l' + G_k'}$

In term of the constructive equation of Modified Kelvin model

$$\{P\} = 1 + p_1' \frac{\partial}{\partial t}、\{Q\} = q_0' + q_1' \frac{\partial}{\partial t}$$

So $\overline{P} = 1 + p_1' s$ $\overline{Q} = q_0' + q_1' s$

According to elastic-viscoelastic correspondence principle

$$\mu_i = \frac{3K_i - 2G_i}{6K_i + 2G_i} \tag{21}$$

$$\overline{G}_i(s) = \frac{\overline{Q}}{\overline{P}} = \frac{2(G_l'G_k' + G_k'\eta_m's)}{G_l' + G_k' + \eta_m's} \tag{22}$$

In addition,

$$z = 0, \qquad \overline{\sigma_z}(s) = \frac{p_z}{s} \tag{23}$$

$$z = H, \qquad \overline{w}(s) = 0 \tag{24}$$

$$r = a, \qquad \overline{\sigma_r}(s) = \frac{p_0 + \gamma_g z}{s} \tag{25}$$

$$r \to \infty, \qquad \overline{\sigma_r}(s) = \frac{\overline{\mu_i}(s)}{s(1-\overline{\mu_i}(s))}(\gamma_0 z + p_z) \tag{26}$$

$$r \to \infty, \qquad \overline{u}(s) = 0 \tag{27}$$

$$\overline{\gamma_0}(s) = \frac{\gamma_0}{s} \tag{28}$$

After Laplace transform, Eqns. (5)-(9) can be rearranged as:

$$\left.\begin{aligned} \overline{u}(s) &= -\frac{1}{4}\frac{a^2}{r}[(\overline{A_1}\gamma_g - \overline{B_1}\gamma_0)z + (\overline{A_1}p_0 - \overline{B_1}p_z)] \\ \overline{w}(s) &= (\overline{C_1}p_z z + \overline{D_1}\gamma_0 z^2 + \overline{F_1}) + [\frac{3a^2}{2}(\overline{X_4}\gamma_0 - \overline{Y_4}\gamma_g) + \overline{L_4}] \end{aligned}\right\} \tag{29}$$

$$\left.\begin{aligned} \overline{\sigma_r}(s) &= \{\overline{I_1}p_z + \overline{I_1}\gamma_0 z + \frac{a^2}{r^2}[(\gamma_g - \gamma_0\overline{I_1})z + (p_0 - p_z\overline{I_1})]\} \\ \overline{\sigma_\theta}(s) &= \{\overline{I_1}p_z + \overline{I_1}\gamma_0 z - \frac{a^2}{r^2}[(\gamma_g - \gamma_0\overline{I_1})z + (p_0 - p_z\overline{I_1})]\} \\ \overline{\sigma_z}(s) &= p_z + \gamma_0 z \\ \overline{\tau_{rz}}(s) &= -\frac{a^2}{2r}(\gamma_g - \gamma_0\overline{I_1}) \end{aligned}\right\} \tag{30}$$

Where

$$\overline{A_1} = \frac{G_l' + G_l' + \eta_m's}{(G_l'G_k' + G_2'\eta_m's)s}$$

$$\overline{B_1} = \overline{A_1} \cdot \frac{1}{s} \cdot \frac{3K_m(G_l' + G_k' + \eta_m' s) - 4(G_l' G_k' + G_k' \eta_m' s)}{3K_m(G_l' + G_k' + \eta_m' s) + 8(G_l' G_k' + G_k' \eta_m' s)}$$

$$\overline{C_1} = \frac{G_l' + G_k' + \eta_m' s}{s[(3K_m G_l' + 3K_m G_k' + 8G_l' G_k') + (3K_m \eta_m' + 8G_k' \eta_m')s]} \quad \overline{D_1} = \frac{G_l' + G_k' + \eta_m' s}{s[(6K_m G_l' + 6K_m G_k' + 16G_l' G_k') + (6K_m \eta_m' + 16G_k \eta_m')s]}$$

$$\overline{F_1} = \frac{G_l' + G_k' + \eta_m' s}{2(G_l' G_k' + G_k' \eta_m' s)} \frac{1}{s}$$

$$\overline{X_4} = \frac{(3K_m G_l' + 3K_m G_k' - 4G_l' G_k') + (3K_m \eta_m' - 4G_k \eta_m')s}{(3K_m G_l' + 3K_m G_k' + 8G_l' G_k') + (3K_m \eta_m' + 8G_k \eta_m')s} \cdot \frac{G_l' + G_k' + \eta_m' s}{(3K_m G_l' + 3K_m G_k' + 2G_l' G_k') + (3K_m \eta_m' + 2G_k' \eta_m')s} \frac{1}{s}$$

$$\overline{Y_4} = \frac{G_l' + G_k' + \eta_m' s}{s[(3K_m G_l' + 3K_m G_k' + 2G_l' G_k') + (3K_m \eta_m' + 2G_k' \eta_m')s]}$$

$$\overline{L_4} = \frac{G_l' + G_k' + \eta_m' s}{2(G_l' G_k' + G_k' \eta_m' s)} \frac{(6K_m G_l' + 6K_m G_k' + 16G_l' G_k') + (6K_m \eta_m' + 16G_k' \eta_m')s}{(3K_m G_l' + 3K_m G_k' + 2G_l' G_k') + (3K_m \eta_m' + 2G_k' \eta_m')s} \frac{1}{s}$$

$$\overline{I_1} = \frac{(3K_m G_l' + 3K_m G_k' - 4G_l' G_k') + (3K_m \eta_m' - 4G_k' \eta_m')s}{s[(3K_m G_l' + 3K_m G_k' + 8G_l' G_k') + (3K_m \eta_m' + 8G_k' \eta_m')s]}$$

Viscoelastic solution was obtained through inverse Laplace transform

$$\left.\begin{aligned} u &= -\frac{1}{4}\frac{a^2}{r}[(A_1 r_g - B_1 \gamma_0) z + (A_1 p_0 - B_1 p_z)] \\ w &= (C_1 p_z z + D_1 \gamma_0 z^2 + F_1) + [\frac{3a^2}{2}(X_4 \gamma_0 - Y_4 \gamma_g) + L_4] \end{aligned}\right\} \tag{31}$$

$$\left.\begin{aligned} \sigma_r &= \{I_1 p_z + I_1 \gamma_0 z + \frac{a^2}{r^2}[(\gamma_g - \gamma_0 I_1) z + (p_0 - p_z I_1)]\} \\ \sigma_\theta &= \{I_1 p_z + I_1 \gamma_0 z - \frac{a^2}{r^2}[(\gamma_g - \gamma_0 I_1) z + (p_0 - p_z I_1)]\} \\ \sigma_z &= p_z + \gamma_0 z \\ \tau_{rz} &= -\frac{a^2}{2r}(\gamma_g - \gamma_0 I_1) \end{aligned}\right\} \tag{32}$$

Where

$$A_1 = \frac{G_l' + G_k'}{G_l' G_k'} - \frac{1}{G_l'} e^{-\frac{G_l'}{\eta_m'} t}, B_1 = V_4 \cdot e^{-(O_6 + Q_6)t} \cdot \cos\{\sqrt{\frac{2(G_l' + G_k')O_6}{G_k'} - (O_6 + Q_6)^2} \cdot t\}$$

$$C_1 = \frac{G_l' + G_k'}{3K_m G_l' + 3K_m G_k' + 8G_l' G_k'}(1 - e^{-\frac{O_6}{2}t}) + \frac{1}{3K_m + 8G_k'} e^{-\frac{O_6}{2}t}, D_1 = \frac{G_l' + G_k'}{6K_m G_l' + 6K_m G_k' + 16G_l' G_k'}(1 - e^{-\frac{O_6}{2}t}) + \frac{1}{6K_m + 16G_k'} e^{-\frac{O_6}{2}t}$$

$$F_1 = \frac{G_l' + G_k'}{2G_k'G_l'}(1 - e^{-\frac{G_l'}{\eta_m'}t}) + \frac{1}{2G_k'}e^{-\frac{G_l'}{\eta_m'}t}$$

$$X_4 = \frac{Q_5}{O_5 - O_4} \cdot (-O_5 \cdot e^{-O_5 t} + O_4 e^{-O_4 t}) + \frac{(S_5 + T_5)}{O_5 - O_4}(e^{-O_5 t} - e^{-O_4 t}) + R_5 + \frac{(O_4 - O_5) - O_4 e^{-O_5 t}}{O_5(O_4 - O_5)O_4} + \frac{O_5 e^{-O_4 t}}{O_5(O_4 - O_5)O_4}$$

$$Y_4 = \frac{G_l' + G_k'}{3K_m G_l' + 3K_m G_k' + 2G_l'G_k'}(1\text{-}e^{-R_7 \cdot t}) + \frac{1}{3K_m + 2G_k'}e^{-R_7 \cdot t}$$

$$L_4 = S_4\{\frac{T_4}{O_4 - Q_4} \cdot (-Q_4 \cdot e^{-Q_4 t} + O_4 e^{-O_4 t}) + \frac{V_4 + (G_l' + G_k')R_4}{O_4 - Q_4}(e^{-Q_4 t} + e^{-O_4 t}) + \frac{(O_4 - Q_4) - O_4 e^{-Q_4 t} + Q_4 e^{-O_4 t}}{Q_4(O_4 - Q_4)O_4}\}$$

$$I_1 = O_7(1 - e^{-\frac{O_6}{2}t}) + Q_7 e^{-\frac{O_6}{2}t}, O_4 = \frac{3K_m G_l' + 3K_m G_k' + 2G_l'G_k'}{3K_m\eta_m' + 2G_k'\eta_m'}, Q_4 = \frac{G_l'}{\eta_m'}, R_4 = 6K_m\eta_m' + 16G_k'\eta_m'$$

$$S_4 = \frac{1}{2G_k'(3K_m\eta_m' + 2G_2'\eta_m')}, T_4 = 6K_m\eta_m' + 16G_k'\eta_m', V_4 = \eta_m'(6K_m G_l' + 6K_m G_k' + 16G_l'G_k')$$

$$O_5 = \frac{3K_m G_l' + 3K_m G_k' + 8G_l'G_k'}{3K_m\eta_m' + 8G_k'\eta_l'} \quad Q_5 = \frac{(3K_m - 4G_k')}{(3K_m + 8G_k')(3K_m + 2G_k')},$$

$$S_5 = \frac{(3K_m - 4G_k')(G_l' + G_k')}{(3K_m + 8G_k')(3K_m + 2G_k')}, T_5 = \frac{(3K_m G_l' + 3K_m G_k' - 4G_l'G_k')}{(3K_m + 8G_k')(3K_m + 2G_k')}, \ V_5 = \frac{3K_m - 4G_k'}{G_k'(3K_m + 8G_k')}$$

$$O_6 = \frac{3K_m G_l' + 3K_m G_k' + 8G_l'G_k'}{6K_m\eta_m' + 16G_k'\eta_m'}, \ Q_6 = \frac{(8G_l' + G_k')(3K_m + 8G_k')}{6K_m G_k'\eta_m' + 16G_k'^2\eta_m'}$$

$$R_6 = (3K_m G_l' + 3K_m G_k' - 4G_l'G_k'), S_6 = (G_l' + G_k')(3K_m - 4G_k'), T_6 = \frac{1}{G_k'(3K_m\eta_m' + 8G_k'\eta_m')}$$

$$V_6 = \frac{G_l' + G_k'}{\eta_m'G_k'}, O_7 = \frac{3K_m G_l' + 3K_m G_k' - 4G_l'G_k'}{3K_m G_l' + 3K_m G_k' + 8G_l'G_k'}, Q_7 = \frac{3K_m - 4G_k'}{3K_m + 8G_k'}, R_7 = \frac{3K_m G_l' + 3K_m G_k' + 2G_l'G_k'}{3K_m\eta_m' + 2G_k'\eta_m'}$$

When serial number of the strata is 1: l=1, k=2, m=1.

When serial number of the strata is 2: l=3, k=4, m=2.

When serial number of the strata is 3: l=5, k=6, m=3.

The viscoelastic solution could be obtained through Laplace transform and inverse Laplace transform based on elastic-viscoelastic correspondence principle [31-32]. The effectiveness of elastic solution has been verified through the comparison of theoretical calculation results and numerical simulation results, which provides the prerequisite of viscoelastic analysis. Moreover, The viscoelastic analysis is in consistency with the standard derivation, which is proposed by Zhou et al [31-32]. Therefore, viscoelastic solution can provide reference for the stability and tightness of underground gas storage carven in bedded salt rock during operation to some extent.

5. CONCLUSION

Considering the characteristics of the salt rock formation in China, mechanical model was simplified into a hollow cylinder, containing non-salt interlayer. Love displacement function was established, which consists of polynomial and logarithmic functions. Based on elastic theory, equations of stress and displacement components were obtained, which contains seven undetermined numbers. Connecting the boundary and the continuity conditions, the value of the coefficient was solved. The elastic general solution was obtained.

The 2D and 3D diagrams of stress and displacement components were drawn utilizing Maple 14 software. The distribution of radius stress and circumferential stress are all similar to parabola, and the value tends to a constant finally. However, the trend of value change is opposite with the change of radius and depth. The continuity of radial displacement is lost in the interlayer. Nevertheless, the maximum value of change is 3.9643mm, which can meet requirement of storage cavern design analysis. To testify the validity of the elastic general solution, the comparison between theoretical calculation and numerical simulation was employed. The theoretical calculation results matches well with the numerical simulation results. The elastic solution can describe the mechanical characteristics of storage cavern in bedded salt rock in elasticity stage well.

Based on the effectiveness elastic solution, viscoelastic solution was obtained through Laplace transform and inverse Laplace transform, which could provide reference for the study on the stability and tightness of underground gas storage carven in bedded salt rock during operation to some extent.

ACKNOWLEDGEMENTS

The research was sponsored by the National Natural Science Foundation of China (grant No. 50874034) and the Science Foundation of Hebei Province (No. E2010000081). The authors gratefully appreciate this support.

CONFLICT OF INTEREST

The authors confirm that this article content has no conflict of interest.

REFERENCE

1. T. Schulze and H. K. Popp, “Development of damage and permeability in deforming rock salt”, Engineering Geology., vol.61, pp.163-180, 2001.
2. C. D. L., Cuevas, L. Miralles, and J. J. Pukyo, “The effect of geological parameters on radiation damage in salt rock: application to salt rock repositories”, Nuclear Technology., vol.114, pp.325-336, 1996.
3. K. Staudtmeister and R. B. Rokahr, “Rock mechanical design of storage caverns for natural gas in salt rock mass”, Int. J. Rock Mech. Min. Sci., vol.34, pp.646, 1997.
4. W. G. Liang, Y. S. Zhao, and S. G. Xu, “Oil and gas storage and nuclear waste disposal in salt rock deposit”, Journal of Taiyuan University of Technology., vol.36, pp.440-443, 2005.
5. C. H. Yang, T. T. Wang, Y. P. Li, H. J. Y, J. J. Li, D. A. Qu, B. C. Xu, Y. Yang, and J.J.K. “Daemen. Feasibility analysis of using abandoned salt caverns for large-scale underground energy storage in China”, Applied Energy., vol.137, pp. 467-481, 2015.

6. P. Bérest and B. Brouard, “Safety of salt caverns used for underground storage blow out; mechanical instability; seepage; cavern abandonment”, Oil Gas Sci. Technol., vol.58, pp.361-384, 2003.
7. Y. Charnavel and N. Lubin, ”Insoluble deposit in salt cavern—test case. Proceedings of SMRI Fall”, In Technical Conference, Bad Ischl, Austria. 2002.
8. G. Crossley and N. Graeme, “Sonar surveys used in gas-storage cavern analysis”, Oil Gas J., vol.96, pp. 96-108, 1998.
9. P. Weidinger, A. Hampel, W. Blum, U. Hunshe, ”Creep behaviour of natural rock salt and its description with the compositemodel.Mater”, Sci. Eng., pp.234-236, 1997.
10. K. H. Lux and S. Heusermann, “Creep tests on rock salt with changing load as a basis for the verify-cation of theoretical material laws,” in Proceeding of 6th Symposium on Salt, 1983, pp. 417-435.
11. W. G. Liang, Y. S. Zhao, and S. G. Xu, “Testing study on physical and mechanical properties of heated salt rock within 240℃”, Chinese Journal of Rock Mechanics and Engineering., vol.23, pp.2365-2369, 2004.
12. W. G. Liang, S. G. Xu, and Y. S. Zhao, “Experimental study on heating recrystallization effect on shear characteristics of damaged rock salt”, Chinese Journal of Rock Mechanics and Engineering., vol.23, pp. 3413-3417, 2004.
13. L. J. Ma, X. Y. Liu, H. F. Xu, R. P. Hua, C H. Li, L. Zhang, and C. Wang, “Deformation and strength properties of rock salt subjected to triaxial compression with cyclic loading”, Chinese Journal of Rock Mechanics and Engineering., vol.32, pp.849-856, 2013.
14. D. E. Munson, and P. R. Dawson, Proc. First Conf. on the Mechanical Behavior of Salt, Trans . Tech. Publications, Clausthal, Germany. 1984.
15. C. J. Peavh, and C. J. Spiers, “Influence of crystal plastic deformation on dilatancy and perme- ability development in synthetic salt rock”. Tectonophysics., vol.256, pp.101-128, 1996.
16. J. C. Stormont, “In-situ gas permeability measurements to delineate damage in rock salt”. International Journal of Rock Mechanic sand Mining Sciences., vol.34, pp.1055-1064, 1997.
17. X. P. Gao, C. H. Yang, W. Wu, and J. Liu, “Experimental studies on temperature dependent properties of creep of rock salt”. Chinese Journal of Rock Mechanics and Engineering., vol.24, pp.2054-2059, 2005.
18. W. G. Liang, S. G. Xu, Y. S. Zhao, and C H. Yang, “Experimental study on creep property of rock salt”, Chinese Journal of Rock Mechanics and Engineering., vol.25, pp.1387-1390, 2006.
19. W. Z. Chen, Z. C. Wang, G. J. Wu, J P. Yang, and B. P. Zhang, “Nonlinear creep damage constitutive model of rock salt and its application to engineering”. Chinese Journal of Rock Mechanics and Engineering., vol.26, pp.467-472, 2007.
20. Y. P. Li, J. Liu, and C. H. Yang, “Influence of mudstone interlayer on deformation and failure characteristics of salt rock”. Chinese Journal of Rock Mechanics and Engineering., vol. 25, pp.2461-2466, 2006.
21. W. Liu, Y. P. Li, D. L. Yin, C. H. Yang, C. Du, X. C. Zhan, and G. M. Zhang, “Analysis of deformation and fracture characteristics of salt rock with tilted interlayer”. Rock and Soil Mechanics., vol.34, pp.645-652, 2013.
22. W. Liu, Y. P. Li, C. H. Yang, H. L. Ma, J. X. Liu, B. W. Wang, and X. L. Huang, “Investigation on permeable characteristics and tightness evaluation of typical interlayer of energy storage caverns in bedded salt rock formations”. Chinese Journal of Rock Mechanics and Engineering., vol.33, pp.500-506, 2014.
23. Y. Li, Q Y. Zhang, C. Jia, J. Liu, S. C. Li, and C. H. Yang, “Fault tree analysis of salt cavern storage during its operational period”. Rock and Soil Mechanics., vol.32, pp.1125-1137, 2011.
24. L. J. Ma, H. F. Xu, M. Y. Wang, and E B. Li, “Numerical study of gas storage stability in bedded rock salt during the complete process of operation pressure runaway”. Chinese Journal of Rock Mechanics and Engineering., vol.34, pp.4108-4115, 2015.
25. S. Ren, X. Y. Li, D. Y. Jiang, X. S. Wang, and C. H. Yang, “Evaluating stability of salt rock gas storage during operation period”. Rock and Soil Mechanics., vol.32, pp.1465-1472, 2011.
26. C. Jia, K. Zhang, Q. Y. Zhang, “Study of time-variant system reliability analytical method for underground salt rock storage group with multiple failure modes during operation period”. Chinese Journal of Rock Mechanics and Engineering., vol.32, pp.926-934, 2013.
27. W. Wang, H. F. Xu, M. Jiang, and Q. Fang, “Theoretical analytical solution of stress distribution in elasticity stage of spherical cavity storage cavern in salt rock”. Chinese Journal of Rock Mechanics and Engineering., vol.31, pp.3731-3739, 2012.
28. Z. H. Zhu, B. G. Wang, and D Z. Guo, Pavement mechanical analysis. Beijing: People’s Communication Press, 1985.
29. Z. L. Xu, Elastic theory. Beijing: People’s Education Press, 1996.
30. G. Q. Zhou and X. M. Liu, Viscoelastic theory. Beijing: Chinese Science and Technology Press ,1996.
31. M. F. Cai, M. C. He, and D. Y. Liu, Rock Mechanics and Engineering. Beijing: Science Press, 2002.
32. G. F. Wang, “Viscoelastic stress analysis of in circlar tunnels”. Engineering mechanics., vol. 7, pp. 106-127, 1990.
33. G..J. Wang and P. Xie, “Theoretical Analysis of Gas and Oil Storage Cavern in Bedded Salt Rock Using a Love Function”. Applied Mechanics and Materials., vol. 204-208 , pp 1499-1502, 2012.